Reprinted from the Journal of the American Ceramic Society, Vol. 70, No. 5, May 1987

Measurement of Residual Stresses in Coatings on Brittle Substrates by Indentation Fracture

MARK F. GRUNINGER,*,* BRIAN R. LAWN,* and EDWARD N. FARABAUGH

Ceramics Division, National Bureau of Standards, Gaithersburg, Maryland 20899

JOHN B. WACHTMAN, JR.*

Center for Ceramics Research, Rutgers University, Piscataway, New Jersey 08854

A method for evaluating stresses in coatings on brittle substrates by indentation is described. The basis for evaluation is a fracture mechanics model of the radial crack system in the Vickers geometry, incorporating the effects of a thin surface stress layer. Experiments on coated glass substrates are used to demonstrate the methodology. The crack sizes on these coated specimens are found to be considerably smaller than those on uncoated controls, indicating substantial (≈50 MPa) in-plane stresses. Substrate tensile stresses, as reflected in the crack expansions observed after applying the coatings to already indented surfaces, are found to make an unexpectedly large contribution to the fracture susceptibility. The procedure offers a simple means for quantifying the mechanical integrity of coating configurations for ceramic components.

I. Introduction

COATINGS are deposited onto substrates not only to change properties but also to offer protection. Such protection can be critical for the mechanical integrity of ceramic components and semiconductor devices, particularly under hostile operating conditions: particulate environments, corrosive atmospheres, thermal cycles, etc., are examples where degradation of properties can be especially severe. With brittle substrates one has to be ever mindful of degradation by fracture processes: in some cases the incidence of a single microcrack can mean failure of a system.

An important element of the protective capacity of coatings is the residual stress state. The stresses in the coating can be substantial.[1,2] There are two main ways in which coating failures can occur, and in both of these ways the residual stresses are envisaged as playing an important role. The first way is by delamination of the coating from the substrate. This possibility has been treated by Evans *et al.*[3–5] in some detail. The second way is by fracture of the overlying coating, where cracks run perpendicular to the free surface through to the substrate. This case has not been treated explicitly in the literature, although Lawn and Fuller foreshadowed it in a recent study of thin-layer stress states.[6] It is this second potential failure mode which is our focus in the present study.

Accordingly, we shall examine the role of residual stresses in coating fracture, using a modification of the earlier Lawn and Fuller treatment. From a practical standpoint, of course, it is the *inhibition* of this kind of failure which may be seen as an ultimate goal, in which case our interest lies primarily with compressive stresses. This interest is confined here to the *measurement* of the stresses, without addressing the separate issue of how such stresses are generated. Our method involves the use of a diamond indenter to introduce a controlled crack pattern into the coated specimen.[7] The stress states are then evaluated from the sizes of the cracks, using comparative measurements on substrates without coatings to establish a reference (zero stress) base line. Independent measurements using thin-beam flexure provide some quantitative confirmation for these evaluations. Glass slides are used as our "standard" brittle substrate, for ease in observing and analyzing the indentation fracture system. However, this should not be construed as restrictive; the technique should be applicable to other brittle substrates with well-behaved indentation fracture behavior. The coating materials are silicon dioxide, silicon nitride, alumina, and zirconia; the typical deposition thickness is 1 μm. The results suggest that the indentation approach could be usefully employed as a (semidestructive) microprobe of coated-surface properties, within certain limitations (most notably those associated with nonideal stress distributions) evident in the data analysis.

II. Indentation Fracture Model of Coating Stress Evaluation

Here we outline the mathematical basis of the indentation fracture method as it applies to a layer/substrate system. Following the earlier analysis,[6] we assume that the surface layer (coating) is thin, such that the dominant stresses are contained *within* this layer. For reasons which will become apparent in Section III, we shall have cause to question this assumption. In particular, we will find evidence to suggest that substrate stresses play a significantly greater role than would be anticipated from analyses based on the notion of an infinitesimally thin coating layer. With this in mind, we consider the fracture mechanics, for Vickers indentation geometry, at three stages of the coating procedure (Fig. 1).

First, consider the crack configuration in an *un*coated, control substrate system (Fig. 1(*A*)). This identifies a convenient zero-stress reference state for data calibration. The key driving force for the radial cracks which grow outward from the impression corners comes from the residual-contact field (associated with elastic-plastic mismatch stresses about the indentation zone).[7–10] For an indentation load, P, the radius, c, of the surface half-penny cracks may be determined from the residual stress intensity factor associated with the residual-contact field

$$K_r = \chi P/c^{3/2} \tag{1}$$

where χ is a dimensionless field intensity parameter.[9] In the post-indentation state the radial cracks can continue to grow subcritically, in air, under the persistent action of K_r, so the traditional toughness parameter, K_c, strictly cannot be used to describe the fracture configurations. The system ultimately comes to "equilibrium" at $K_r = K_c'$, where K_c' ($<K_c$) is a threshold point on the v-K curve, i.e., a point where the crack velocity diminishes to zero.[11] For this equilibrium state, Eq. (1) may be rearranged to give

$$P/c_I^{3/2} = K_c'/\chi = \text{constant} \tag{2}$$

where the subscript I is to denote specifically our first (reference) coating configuration. A test of the indentation theory is therefore that $P/c_I^{3/2}$ should be crack-size invariant.[12]

The second configuration relates to a system *with* coating, but specifically for deposition *after* indentation of the substrate

Presented at the 88th Annual Meeting of the American Ceramic Society, Chicago, IL, April 29, 1986 (Basic Science Division, Paper No. 93-B-86). Received June 2, 1986; revised copy received November 10, 1986; approved December 16, 1986.

Supported in part by the U.S. Office of Naval Research, Metallurgy and Ceramics Program.

*Member, the American Ceramic Society.

*Work done while on leave from Rutgers University.

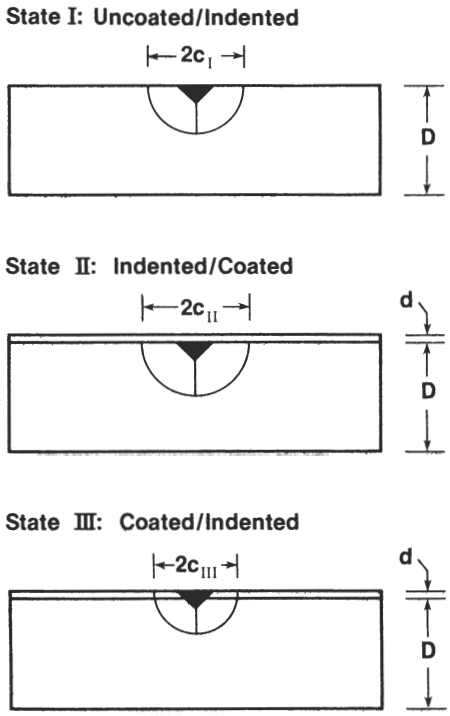

Fig. 1. Vickers indentation, for three stages of coating: (*A*) indentation of uncoated substrate; (*B*) indentation of substrate, followed by coating; (*C*) coating of substrate, followed by indentation. Shown here for compressive coating stress, tensile substrate stress. Dimension c represents surface crack radius, d coating thickness, and D substrate thickness.

(Fig. 1(*B*)). (It is implicit here that the coating maintains its integrity across the crack mouth.) Since in this case the cracks are contained entirely in the substrate, they should differ in size from those in configuration I *only* if the substrate stresses are significant. Conversely, any differences in the crack sizes in configurations I and II should allow us to evaluate the substrate stress contribution. To formalize this notion, let us write the net stress intensity factor acting on the radial crack system as

$$K = K_r + K_s \tag{3}$$

where the substrate term $K_s = K_s(c)$ is some function of crack size. At equilibrium, $K = K_c'$, Eq. (3) may be rearranged to give the configuration II relation

$$P/c_{\mathrm{II}}^{3/2} = (K_c' - K_s)/\chi \tag{4a}$$

$$= (P/c_{\mathrm{I}}^{3/2})[1 - K_s(c_{\mathrm{II}})/K_c'] \tag{4b}$$

where we have invoked Eqs. (1) and (2) to eliminate K_r and χ. Note that now the quantity $P/c_{\mathrm{II}}^{3/2}$ will not be crack-size invariant (unless K_s just happens to be independent of c).

To proceed beyond this point, so that we may establish a quantitative basis for subsequent evaluation of the substrate term, let us consider the idealistic case of a uniform substrate stress, σ_s. We might expect this to be a reasonable approximation for a very thin coating (i.e., $d \ll c$, Fig. 1) with a perfectly abrupt interface at the substrate (e.g., no interdiffusion of material across the interface). Then we may write

$$K_s = \psi\sigma_s c^{1/2} \tag{5}$$

where ψ is a dimensionless crack geometry term of order unity. In this approximation Eq. (4*b*) becomes

$$P/c_{\mathrm{II}}^{3/2} = (P/c_{\mathrm{I}}^{3/2})[1 - (\psi\sigma_s/K_c')c_{\mathrm{II}}^{1/2}] \tag{6}$$

Equation (6) predicts an increasing departure from the reference state value of $P/c_{\mathrm{I}}^{3/2}$ as crack size increases.

Configuration III (Fig. 1(*C*)) corresponds to a system with coating, as in configuration II, but this time for deposition *before* indentation of the substrate. The cracks are now expected to extend into the coating, and thereby to experience driving forces associated with the coating stresses as well as the substrate stresses (although these driving forces will inevitably oppose each other because the net section forces must balance out). Then provided the essential pennylike geometry of the cracks is preserved (questionable, especially in view of the nonaxial symmetry of the stress distribution),[13] Eq. (3) may be further generalized to include a thin-film contribution, K_f

$$K = K_r + K_s + K_f \tag{7}$$

In conjunction with Eqs. (1) to (6), and with the equilibrium requirement $K = K_c'$, this relation may be rearranged to give, for configuration III

$$P/c_{\mathrm{III}}^{3/2} = (K_c' - K_s - K_f)/\chi \tag{8a}$$

$$= (P/c_{\mathrm{I}}^{3/2})[1 - \psi\sigma_s c_{\mathrm{III}}^{1/2}/K_c' - K_f(c_{\mathrm{III}})/K_c'] \tag{8b}$$

Implicit in this formulation is the assumption that the sole influence of the coating lies in its stress state. The fact that the fracture properties of the coating *material* may differ from those of the substrate is neglected, in the spirit of the thin-film approximation (see Appendix A).

In this same spirit, Lawn and Fuller[6] calculated the thin-film stress intensity factor in the form

$$K_f = 2\psi\sigma_f d^{1/2} \tag{9}$$

with ψ the same as in Eq. (5). Note that K_f is independent of crack size here. Now, Eq. (8*b*) may be written in more explicit form

$$P/c_{\mathrm{III}}^{3/2} = (P/c_{\mathrm{I}}^{3/2})[(1 - 2\psi\sigma_f d^{1/2}/K_c') - (\psi\sigma_s/K_c')c_{\mathrm{III}}^{1/2}] \tag{10}$$

Equations (2), (6), and (10) provide us with the basis for a complete stress evaluation, within the bounds of the approximations used, from $c(P)$ data for the three coating/indentation sequences.

III. Experimental Procedure and Results

Indentation fracture experiments were made on soda-lime glass substrates before and after coating, in accordance with the configurational states represented in Fig. 1. The substrates for the indentation studies were microscope slides, 1 mm thick. Additional substrates of the same material were prepared to 0.15-mm thickness for comparative study by thin-beam deflection. The substrates were preannealed at 520°C for 1 h to remove any preexisting surface stresses (as confirmed by observing the complete disappearance of residual stress birefringence around "dummy" indentations in the slides). Coatings were applied to the upper side of the substrates by either radio-frequency diode sputtering (silicon dioxide, silicon nitride, alumina) or electron beam deposition (zirconia) to thicknesses in the range 0.7 to 2.0 μm. Indentations were made using a Vickers diamond pyramid at loads of 10 to 50 N, such that well-developed radial crack patterns were obtained in all cases (i.e., surface crack dimension >2 times the hardness dimension, without chipping[14]). These indentations were made in air, with a load hold time of 15 s, and allowed to equilibrate for 1 d before measurement.[11] (No significant crack growth was observed after this aging time.) Mean crack sizes c were determined from 6 to 8 indentations at each load P, to obtain standard deviation limits in $P/c^{3/2}$ values, for any given coating/substrate crack configuration.

A precautionary check was conducted on the impression sizes (as distinct from the crack sizes), to ensure that the hardness remained relatively insensitive to the coating/substrate stress state. (Note that the elastic-plastic parameter χ in Eqs. (2), (4), and (8) is implicitly assumed to be invariant.) No distinguishable difference in the measured hardness (5.5 ± 0.3 GPa) could be detected between the configurations of Fig. 1.

During the course of the indentation measurements a telling

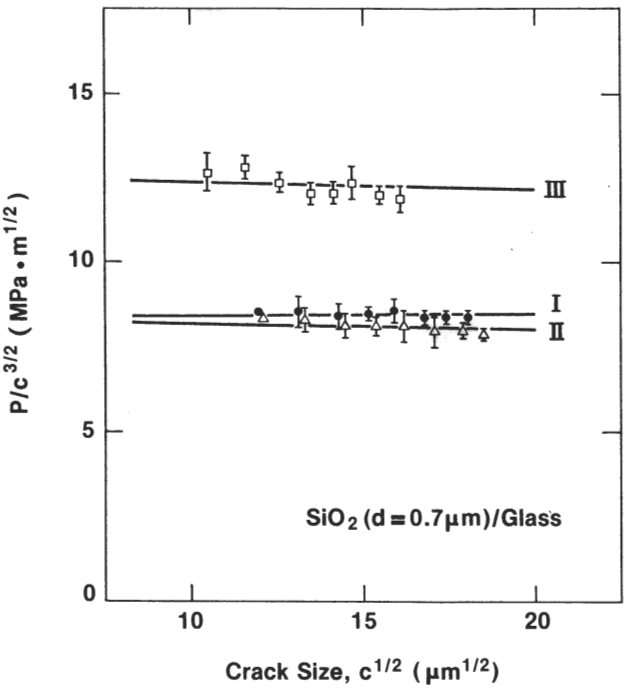

Fig. 2. Plots of $P/c^{3/2}$ vs $c^{1/2}$ for SiO_2 coating on soda-lime glass substrate. States I, II, and III correspond to those represented in Fig. 1.

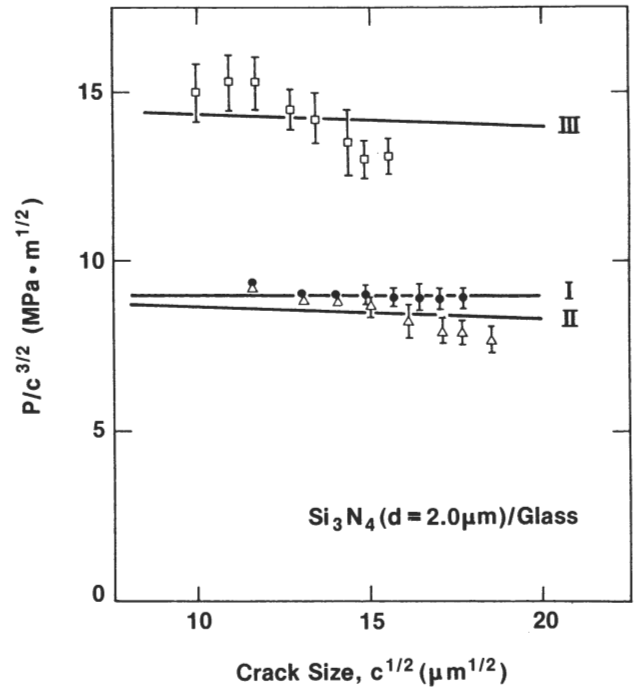

Fig. 3. Plots of $P/c^{3/2}$ vs $c^{1/2}$ for Si_3N_4 coating on soda-lime glass substrate.

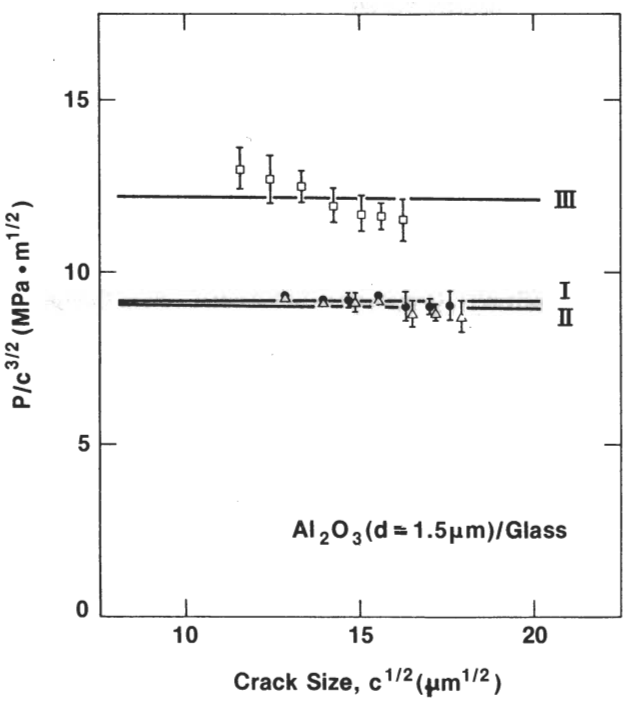

Fig. 4. Plots of $P/c^{3/2}$ vs $c^{1/2}$ for Al_2O_3 coating on soda-lime glass substrate.

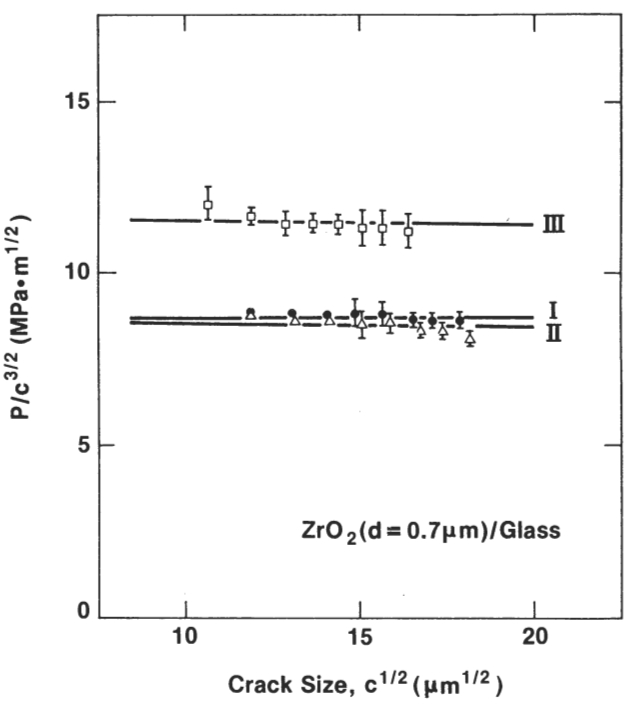

Fig. 5. Plots of $P/c^{3/2}$ vs $c^{1/2}$ for ZrO_2 coating on soda-lime glass substrate.

observation was made concerning the state of the glass surfaces. These surfaces developed shallow, but clearly visible, fissure patterns after deposition of the (transparent) coating. The patterns were strongly reminiscent of those produced in glass after ion-exchange[15] or particle-irradiation[6] treatments. In those cases the patterns were attributed to surface-localized growth of incipient flaws under the action of an induced tensile stress layer. It thus seemed apparent that a similar state of localized tensile stress must exist in our coated substrates. Hence the inclusion of the K_s term in Eqs. (3) and (4).

Figures 2 to 5 show plots of the measured $P/c^{3/2}$ values as a function of square root of crack size for the four coating materials. In each of these four cases the entire set of results for states I, II, and III (Fig. 1) was obtained from a single glass slide, to ensure self-consistency in data comparisons. (Some error bars are omitted from these data plots where overlap of points occurs.) Let us consider the general data trends for states I, II, and III in turn.

State I: The quantity $P/c_1^{3/2}$ for uncoated substrates is, within experimental scatter, independent of crack size, consistent with Eq. (2). The horizontal straight lines through these points represent

Table I. Calculated Stresses for Coatings (Figs. 2 to 5) on Soda-Lime Glass Substrates*

Coating material	d (μm)†	σ_s (MPa)‡ (Indentation)	σ_f (MPa)§	
			Indentation	Deflection
SiO_2	0.7	0.6 ± 0.3	−72.6 ± 5.9	−87.4 ± 8.7
Si_3N_4	2.0	1.0 ± 0.8	−55.9 ± 8.9	−46.1 ± 5.0
Al_2O_3	1.5	0.2 ± 0.2	−34.4 ± 6.1	
ZrO_2	0.7	0.4 ± 0.3	−50.8 ± 4.5	

*Errors quoted are standard deviation limits. †Thickness. ‡Substrate stress. §Coating stress.

mean value levels, establishing zero-stress reference base lines for the remaining two states.

State II: The data points $P/c_{II}^{3/2}$ for indented/coated substrates are not independent of crack size, but deviate increasingly below the state I reference line as crack size increases. This indicates, from Eq. (4*b*), that the K_s term is non-zero, is positive (tensile), and, in qualitative agreement with Eq. (5), is an increasing function of c. From a *quantitative* standpoint, Eq. (6) predicts a linear plot against the $c^{1/2}$ coordinate, with intercept $P/c_I^{3/2}$ (i.e., lines I and II intersecting at $c = 0$) and slope $-(P/c_I^{3/2})(\psi\sigma_s/K_c')$. The lines through the state II data points in Figs. 2 to 5 are the best force fits in accordance with this predicted response. There appear to be systematic departures from these fits, indicating that the assumptions underlying the theory are not strictly valid. Notwithstanding these departures, the analysis provides us with the means for obtaining at least an approximate estimate of the substrate stresses.

State III: The corresponding data points $P/c_{III}^{3/2}$ for coated/indented substrates lie well *above* the state I reference line, indicative of a relatively large compressive stress on the crack system from the coating. Again, these plots incline downward at increasing crack size, in similar fashion to those for state II, consistent with the persistence of the substrate K_s term in Eq. (8). More specifically, Eq. (10) again predicts a linear plot against $c^{1/2}$, with the same slope $-(P/c_I^{3/2})(\psi\sigma_s/K_c')$ as determined from the state II data (i.e., line III parallel to line II) and intercept $(P/c_I^{3/2})\cdot(1 - 2\psi\sigma_s/K_c')$. The lines through the state III data in the figures are appropriate best force fits. With the same reservations concerning systematic departures as above, we now have the basis for evaluating the coating stresses.

Accordingly, taking $\psi \approx 1$ for the radial crack system[16] and $K_c' \approx 0.25$ MPa·m$^{1/2}$ as the threshold stress intensity factor for soda-lime glass in air,[11] we obtain the values of σ_s and σ_f shown in Table I for the four coating systems studied.

The values of σ_f thus obtained may be compared in Table I with those from independent measurements by a conventional thin-beam deflection procedure (Appendix B), for similar SiO_2 and Si_3N_4 coatings on the *thinner* (0.15 mm) glass substrates. (In this context it may be mentioned that the same technique was unable to resolve any bending of the thicker (1 mm) substrates used in the indentation tests, indicating that the stress values σ_s quoted in Table I are not due to specimen bending.) The results from the two sets of stress measurement appear to be quantitatively consistent.

IV. Discussion

We have described a method for evaluating thin-layer stresses for coatings on brittle substrates. The procedure is simple, as is characteristic of the general indentation testing methodology.[7] There is evidence for systematic departure from the assumptions which underlie the theoretical formulation (about which we shall say more below), in which case we need to be careful before attaching too much significance to the absolute values quoted in Table I. However, provided we ensure constancy in the experimental indentation testing conditions (e.g., load range), we may be confident in the accuracy of *relative* stress measurements. Thus the method should be valuable in investigating the effects of changes in the coating material (as in Figs. 2 to 5), substrate material (with the proviso that this material produces well-defined radial crack patterns), coating thickness, and so on.

The experimental results reveal that substrate stresses are by no means negligible in the configurations studied here. They are apparently of sufficient magnitude to bias the $P/c_{II}^{3/2}$ and $P/c_{III}^{3/2}$ data in Figs. 2 to 5 noticeably away from horizontal plots (as would be predicted for $\sigma_s = 0$ in Eqs. (6) and (10)). In fact, the values of σ_s in Table I are somewhat greater than we would anticipate from a simple section force balance argument,[1,13] i.e., $\sigma_s = -\sigma_f d/D$ for zero bending (i.e., for $d \ll D$, Fig. 1). This suggests that our in-built assumption of uniformly distributed stresses on either side of an infinitesimally thin interface may not be entirely applicable. On the other hand, these substrate stresses are somewhat less than those that we would ordinarily expect to be necessary to cause surface cracks (Section III) to propagate in glass (typical strengths, 10 to 100 MPa). It is conceivable that herein lies the cause of the systematic departures referred to above.

Our allusions here to certain limitations in the stress evaluation methodology should not be taken as detracting from the practical usefulness of the indentation microprobe as a potential predictor of in-service performance. After all, the indentation fracture system closely simulates the kind of damage that brittle surfaces suffer from incidental contacts with particulate matter which pervades the typical operating environment.[17] As such, the evaluations described here should serve as a most appropriate quantitative indicator of the protective capacity of thin coatings against erosion, wear, and ultimate failure of ceramic components.

APPENDIX A

Effective Toughness of Substrate/Coating Composite

In the derivations leading to Eq. (8) it is implicitly assumed that the coating influences the indentation pattern by virtue of its stress state but *not* by its fracture properties. We present a simplistic derivation here to justify this assumption.

Consider the crack configuration in Fig. 1(*C*). Designate the environmentally influenced "toughness" of the substrate and the film as $K_c^{s\prime}$ and $K_c^{f\prime}$, respectively. Our aim is to find an expression for the "effective" toughness K_c', in terms of $K_c^{s\prime}$ and $K_c^{f\prime}$, which represents the substrate/coating composite.

To do this we write, in the usual way, the relations between toughnesses, K_c, Young's moduli, E, and surface energies, γ:

$$K_c' = (2E\gamma')^{1/2} \tag{A-1a}$$

$$K_c^{s\prime} = (2E_s\gamma_s')^{1/2} \tag{A-1b}$$

$$K_c^{f\prime} = (2E_f\gamma_f')^{1/2} \tag{A-1c}$$

For an incremental crack extension, δc, the corresponding increase in effective surface energy (recalling that there are *two* crack walls, but that we are dealing with a *half*-penny crack) is

$$\pi\gamma' c\,\delta c = \pi\gamma_s' c\,\delta c + 2d(\gamma_f' - \gamma_s')\,\delta c \tag{A-2}$$

Thus we have

$$\gamma' = \gamma_s' + (2d/\pi c)(\gamma_f' - \gamma_s') \tag{A-3}$$

Using the same kind of incremental area argument we arrive at an analogous expression for the composite modulus:

$$E = E_s + (2d/\pi c)(E_f - E_s) \tag{A-4}$$

Thus, combining Eqs. (A–3) and (A–4) with Eq. (A–1) we obtain

$$K_c' = K_c^{s\prime}\{[1 + (2d/\pi c)(E_f/E_s - 1)] \times [1 + (2d/\pi c)\{(E_s/E_f)(K_c^{f\prime}/K_c^{s\prime})^2 - 1\}]\}^{1/2} \quad \text{(A–5)}$$

For the "worst case" encountered in our experiments, i.e., for low load indentations in Al_2O_3/glass, $E_f/E_s = 400$ GPa/70 GPa, $K_f'/K_s' = 1.0$ MPa·m$^{1/2}$/0.25 MPa·m$^{1/2}$ (threshold K values on v-K curves),[18] $d/c = 1.5$ μm/150 μm, we have $K_c' = 1.03K_c^{s\prime}$. That is, the effective toughness *generally* differs from the substrate toughness by <3%, which we take to be negligible.

APPENDIX B

Stress Measurement by Thin-Beam Deflection

A commonly used method for measuring coating stresses is that of beam deflection.[1,19,20] With this method the substrate must be thin enough, relative to the coating thickness, that the coating stresses can cause measurable curvatures in the specimens. In our case it was necessary to go from the 1-mm-thick slides used for the indentation test to 0.15-mm-thick polished bar sections to obtain sufficient accuracy in stress evaluation.

The conditions of our deflection experiments were as follows. The specimens were coated with SiO_2 or Si_3N_4, as indicated in the text. Low-load (9 mg) stylus profilometry was used to measure the radii of curvature, R_0 and R, before and after coating. The coating stresses were then evaluated from the flexure formula[20]

$$\sigma_f = [E_s D^2/6(1 - \nu)d](1/R - 1/R_0) \quad \text{(B–1)}$$

to an accuracy of about 10%.

Acknowledgments: The assistance of K. H. Hatton and R. H. Steiner in preparing the coated specimens is gratefully acknowledged.

References

[1]R. W. Hoffman; pp. 273–353 in Physics of Non-Metallic Thin Films. Edited by C. H. S. Dupuy and A. Cachard. Plenum, New York, 1976.
[2]H. K. Pulkar, Coatings on Glass. Elsevier, Amsterdam, 1984.
[3]A. G. Evans and J. W. Hutchinson, "On the Mechanics of Delamination and Spalling in Compressed Films," *Int. J. Solids Struct.*, **20** [5] 455–66 (1984).
[4]D. B. Marshall and A. G. Evans, "Mechanics of Adherence of Residually Stressed Thin Films by Indentation: I. Mechanics of Interface Delamination," *J. Appl. Phys.* **56** [10] 2632–38 (1984).
[5]C. Rossington, A. G. Evans, D. B. Marshall, and B. T. Khuri-Yakub, "Measurements of Adherence of Residually Stressed Films by Indentation: II. Experiments with ZnO/Si," *J. Appl. Phys.*, **56** [10] 2639–44 (1984).
[6]B. R. Lawn and E. R. Fuller, "Measurement of Thin-Layer Surface Stresses by Indentation Fracture," *J. Mater. Sci.*, **19** [12] 4061–67 (1984).
[7]D. B. Marshall and B. R. Lawn; pp. 26–46 in Micro Indentation Techniques in Materials Science and Engineering. Edited by P. J. Blau and B. R. Lawn. A.S.T.M. Special Technical Publication 889, Philadelphia, 1986.
[8]D. B. Marshall and B. R. Lawn, "Residual Stress Effects in Sharp-Contact Cracking: I. Indentation Fracture Mechanics," *J. Mater. Sci.*, **14** [9] 2001–12 (1979).
[9]B. R. Lawn, A. G. Evans, and D. B. Marshall, "Elastic/Plastic Indentation Damage in Ceramics: The Medial/Radial Crack System," *J. Am. Ceram. Soc.*, **63** [9–10] 574–81 (1980).
[10]E. R. Fuller, B. R. Lawn, and R. F. Cook, "Theory of Fatigue for Brittle Flaws Originating from Residual Stress Concentrations," *J. Am. Ceram. Soc.*, **66** [5] 314–21 (1983).
[11]B. R. Lawn, K. Jakus, and A. C. Gonzalez, "Sharp vs Blunt Crack Hypotheses in the Strength of Glass: A Critical Study Using Indentation Flaws," *J. Am. Ceram. Soc.*, **68** [1] 25–34 (1985).
[12]T. P. Dabbs, B. R. Lawn, and P. L. Kelly, "A Dynamic Fatigue Study of Soda-Lime Silicate and Borosilicate Glasses Using Small-Scale Indentation Flaws," *Phys. Chem. Glasses*, **23** [2] 58–66 (1982).
[13]B. R. Lawn and D. B. Marshall, "Contact Fracture Resistance of Physically and Chemically Tempered Glass Plates: A Theoretical Model," *Phys. Chem. Glasses*, **18** [1] 7–18 (1977).
[14]G. R. Anstis, P. Chantikul, B. R. Lawn, and D. B. Marshall, "A Critical Evaluation of Indentation Techniques for Measuring Fracture Toughness: I. Direct Crack Measurements," *J. Am. Ceram. Soc.*, **64** [9] 533–38 (1981).
[15]F. M. Ernsberger, "Detection of Strength-Impairing Surface Flaws in Glass," *Proc. R. Soc. London*, **A257** [1289] 212–23 (1960).
[16]D. B. Marshall and B. R. Lawn, "Flaw Characteristics in Dynamic Fatigue: The Influence of Residual Contact Stresses," *J. Am. Ceram. Soc.*, **63** [9–10] 532–36 (1980).
[17]B. R. Lawn, D. B. Marshall, P. Chantikul, and G. R. Anstis, Indentation Fracture: Applications in the Assessment of Strength of Ceramics," *J. Aust. Ceram. Soc.*, **16** [1] 4–9 (1980).
[18]B. R. Lawn, D. H. Roach, and R. M. Thomson, "Thresholds and Reversibility in Brittle Cracks"; to be published in *J. Mater. Sci.*
[19]A. G. van Nie, "A Method for the Determination of the Stress in and Young's Modulus of Silicon Nitride Passivation Layers," *Solid State Technol.*, **23** [1] 81–84 (1980).
[20]C. M. Drum and M. J. Rand, "A Low Stress Insulating Film on Silicon by Chemical Vapor Deposition," *J. Appl. Phys.*, **39** [9] 4458–59 (1968). □